

Circumstellar structures in the eclipsing binary β Lyr A

Gasdynamical modelling confronted with observations

D.V. Bisikalo¹, P. Harmanec², A.A. Boyarchuk¹, O.A. Kuznetsov³, and P. Hadrava²

¹ Institute of Astronomy, Russian Academy of Sciences, Pyatnitskaya 48, Moscow 109017, Russia
(bisikalo@inasan.rssi.ru; aboyar@inasan.rssi.ru)

² Astronomical Institute, Academy of Sciences of the Czech Republic, 251 65 Ondřejov, Bohemia, Czech Republic
(hec@sunstel.asu.cas.cz; had@sunstel.asu.cas.cz)

³ Keldysh's Institute of Applied Mathematics, Miusskaya Square 4, Moscow 125047, Russia (kuznecov@spp.keldysh.ru)

Received 8 June 1999 / Accepted 9 November 1999

Abstract. A disentangling technique was applied to obtain an independent check on the amplitude of the radial-velocity curve of the more massive component of β Lyr derived earlier. This is crucial for the reliable determination of the component masses and their separation. Currently the best available basic physical properties of the binary were then defined. For them, 3-D gasdynamical simulations of mass transfer between the binary components of β Lyr were calculated and confronted with the existing evidence of various circumstellar structures within the binary system. It turns out that the gasdynamical model is able to explain, in principle, the formation of the basic observed components of the circumstellar matter. This brings us one step farther to the understanding of this unusual object.

Key words: stars: emission-line, Be – stars: binaries: eclipsing – stars: binaries: spectroscopic – stars: binaries: visual – stars: individual: – techniques: spectroscopic

1. Introduction

The ever challenging eclipsing and spectroscopic binary β Lyr has been observed by various techniques for over the past 200 years. A good and detailed review of the historical studies of β Lyr was published by Sahade (1980) and later extended by Plavec (1985), Harmanec (1990), Harmanec & Scholz (1993) and Harmanec et al. (1996).

β Lyr (10 Lyr, HR 7106, HD 174638, BD+33°3223, ADS 11745A) is the brightest member (component A) of an optical system of six stars and a 12.9-d spectroscopic and eclipsing binary with ample evidence of circumstellar matter within and around the system. The binary is at a distance of (270 ± 39) pc from us according to Perryman et al. (1997) and Linnell et al. (1998) and consists of the following two stars: (1) the more massive *star 1* (probably of an early-B spectral type) which is completely (or almost completely) hidden from view by a thick accretion disc, and (2) the less massive B6-8II *star 2*

which, however, is the brighter of the two in the optical region. This is so because of its large radius and because the light of *star 1* is obscured by the circumstellar disc and re-radiated away from the orbital plane. The binary orbit is circular and the primary eclipse of *star 2* by *star 1* and its disc is about $1^m.0$ deep in the visual; the secondary eclipse is $0^m.5$ deep. Due to combined effects of the ellipticity of *star 2* and the presence of a thick disc, the light curve has no flat portions. The orbital period has been growing at a rate of 19 s per year. Currently the best available ephemeris was derived by Harmanec & Scholz (1993) and reads as follows:

$$T_{\text{prim.eclipse}} = (\text{HJD } 2408247.966 \pm 0.018) + (12^d.913780 \pm 0^d.000020) \times E + (3.8720 \pm 0.0051) 10^{-6} \times E^2. \quad (1)$$

In this paper, we attempted to define the most probable basic physical properties of the binary, calculate for them a 3-D gasdynamical model of the gas flow in β Lyr and confront the results with the existing observations of circumstellar matter in this binary.

2. Structure of circumstellar matter in β Lyr

2.1. Line spectrum of β Lyr

According to current knowledge, at least six different systems of spectral lines are observed in the IR, optical and UV spectra of β Lyr:

1. **The B6-8II spectrum:** Strong and relatively sharp ($v \sin i = 50 - 60 \text{ km s}^{-1}$) absorption lines of *star 2*, visible at all orbital phases, which define its radial-velocity (RV hereafter) curve with a full amplitude of 370 km s^{-1} , first derived by BÉlopolsky (1893a), BÉlopolsky (1893b).
2. **The B-type “shell” absorption spectrum:** The main absorption components of He I lines, Balmer lines and many metallic lines define an absorption spectrum which was originally classified as B2 or B5 and was believed to belong to *star 1*. However, already Struve (1934) pointed out that the

spectrum is peculiar and cannot originate in a stellar photosphere but in circumstellar matter. This is also supported by the fact that the individual lines are all blue-shifted for various amount up to 200 km s^{-1} (this shift varies from line to line) and stronger lines have several components with different RVs. Numerous absorption lines observed in the satellite UV spectra of β Lyr show very similar patterns of behavior as described above for the optical shell lines. This is also true for the strong resonance lines of ions like C IV or Si IV. The structure of these lines varies not only with the orbital phase but also on different time scales. Very clear cycle-to-cycle variations of the He I 6678 line were demonstrated by Harmanec et al. (1996) - see their Fig. 14.

3. **The emission spectrum:** Strong emission lines of H I and He I and weaker metallic emission lines, numerous also in the satellite UV spectra, vary in intensity both with the orbital phase and secularly. The RV measured on the wings of these lines follows a sinusoidal RV curve with an amplitude of about 30 km s^{-1} which does not coincide with the orbital motion of either binary component and attains its maximum at orbital phase $0^{\text{P}}.30$. Struve (1941) noted a clear correspondence between the emission spectrum and the shell spectrum mentioned above.
4. **The satellite spectrum:** Strong additional absorption lines are observed only in narrow phase intervals before and after the primary mid-eclipse (of *star 2* by *star 1* and its disc). They are red-shifted before, and blue-shifted after the mid-eclipse, in both cases for some 200 km s^{-1} . According to Sahade et al. (1959), the red-shifted lines correspond to a spectral class A2 while the blue-shifted lines are of a somewhat earlier spectral type.
5. **Secondary Si II 2 absorption spectrum:** First noted by Sahade (1966), this pair of weak absorption lines was studied by Skulskij (1975), Skulskij & Topilskaya (1991) and Skulskij (1992) who found that their RV varies in an exact anti-phase to the RV curve of *star 2* and interpreted them as *photospheric* lines from the atmosphere of *star 1*. Harmanec (1992) re-interpreted these lines as *shell* lines from the disc around *star 1* but maintained Skulskij's conclusion that they represent the best available estimate of the true orbital motion of *star 1*.
6. **The interstellar lines:** Sharp and quite strong lines of Ca II or Si II are observed with a RV of some -17 km s^{-1} . This value is identical to the systemic velocity of the β Lyr system. The possibility that the observed lines are mainly circumstellar cannot, therefore, be excluded without further dedicated studies at very high resolution.

2.2. Evidence of circumstellar matter

The presence of circumstellar matter in β Lyr is documented by at least four, and possibly five of the above discussed systems of spectral lines:

- by the emission lines, observed invariably since the first visual spectroscopic observations of β Lyr by Secchi (1867);

- by the B-type shell lines;
- by the A-type shell lines observed in Si II 2 in all orbital phases and in the so-called satellite lines near the primary eclipse; and possibly
- by the circumstellar lines of Ca II and Si II.

Besides that, there is also evidence from continuum radiation: Jameson & King (1978) modelled the radio emission from β Lyr as originating from a H II region around the system and Berghöfer & Schmitt (1994) reported X-ray emission from β Lyr.

2.3. Current understanding of the circumstellar matter

Already Curtiss (1911) considered a model in which *star 1* was enclosed by an extended gaseous envelope. The satellite lines were correctly interpreted as lines from the circumstellar envelope around *star 1* projected against disc of *star 2* by Baxandall et al. (1930). According to them, they were due to "circulating currents in the outer envelope". This can now be viewed as the very first report of the existence of an accretion disc.

According to Harmanec et al. (1996), most of the emission originates in bipolar jet-like structures which emanate from an area of probable interaction of the gas stream from *star 2* towards *star 1* with the disc around *star 1*. Independently, such structures were found from spectropolarimetry by Hoffman et al. (1998). Harmanec et al. (1996) tentatively suggested that the B-type "shell" absorption lines originate from self-absorption in one of the jets. Given the estimated orbital inclination of the binary system, the blue shift of $100 - 200 \text{ km s}^{-1}$ translates into true outflow velocities of the order of 1000 km s^{-1} , quite typical for the wind velocities of early-type stars.

Recently, Linnell et al. (1998) attempted to model both, the observed light curves and the phase variations of the observed continuum radiation of β Lyr assuming the presence of radiation from two stellar bodies and a self-consistently treated accretion disc around *star 1* but neglecting the jet-like structures. Such an assumption seems justified since no observable effects of the jet-like structures on the observed light curves were found and it is conceivable that these structures only affect the line radiation. However, the conclusion of Linnell et al. (1998) is that it is not possible to describe both, the continuum shape changes and the observed light curves from UV to optical regions by one set of physical parameters. Their conclusion is that there must also be a hot, electron-scattering region above and below the disc around *star 1*. Note that such a region was independently postulated by Burnashev & Skulskij (1978) who, however, interpreted *star 1* as an A5III star. Linnell et al. (1998) also confirmed an earlier conclusion of Wilson (1974) that the radiation of *star 1* is *completely* obscured by the disc.

3. An attempt at KOREL decomposition of the spectrum

The determination of all basic physical properties of the β Lyr system depends critically on the RV curve of *star 1* derived by Skulskij and his collaborators from the RV measurements of the

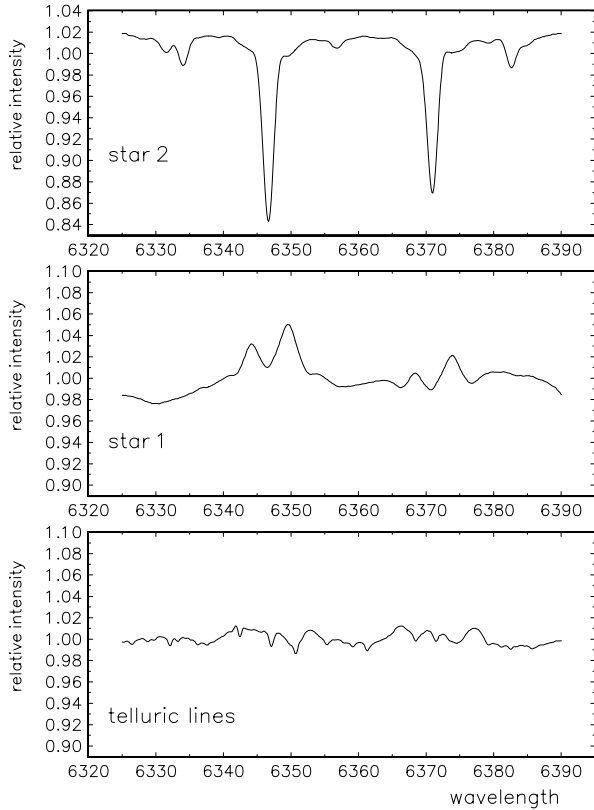


Fig. 1. Decomposed line profiles of both binary components of β Lyr and of the telluric spectrum in the neighbourhood of Si II 2 lines

weak pair of Si II 2 lines (see above). It was, therefore, deemed useful to obtain this RV curve also from an independent set of spectroscopic observations and using an objective method. Note that the Si II 2 lines consist of a blend of two absorption components (from *star 2* and disk around *star 1*), Si II emission and telluric lines. Skulskij made a kind of ‘manual’ rectification to remove the effects of the emission prior to RV measurements. However, he could not measure the position of both absorption components reliably at phases near conjunctions where the two lines blend with each other. We, therefore, decided to apply a disentangling technique. The computer program KOREL for spectral disentangling and relative line photometry, developed by Hadrava (1995, 1997), was used. No doubt, the application of KOREL to the Si II 2 lines of β Lyr has some problems of its own: The method is based on the assumption that the line profiles of both binary components *do not change their shape* with the orbital phase. It is almost certain that this assumption is violated in the case of β Lyr. KOREL can, however, allow for changing line intensities and this option was used during our attempts at the orbital solution and our current experience with this method is that it is quite robust with respect to non-orbital ‘noise’ in the line profiles. There is some hope, therefore, that average line profiles and the resulting RV curves can be considered meaningful. Since the disentangling techniques are developing rapidly, it is also of some interest to see the performance of KOREL in a complicated case.

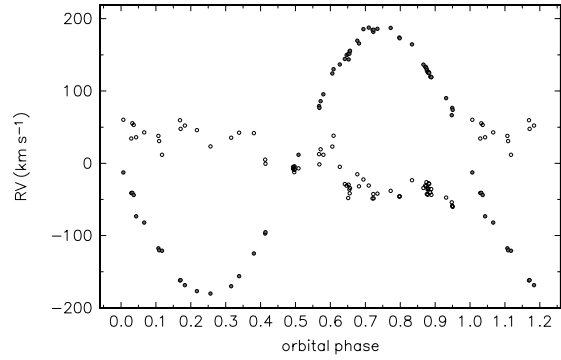


Fig. 2. RV curves of both binary components of β Lyr which resulted from KOREL disentangling orbital solution presented here; open circles correspond to the RV curve of *star 1*

KOREL was applied to a selection of 68 Ondřejov reticon spectra with the best S/N from the data set, used earlier by Harmanec et al. (1996). The spectral region between 6325 Å and 6390 Å, covering both Si II lines (at 6347 and 6371 Å), has been decomposed into two components in a circular orbit, defined by ephemeris 1, and into telluric spectrum. The orbit of the Earth around the Sun was kept fixed at known values. The radial velocities and strengths of the telluric lines were first converged separately in the spectral region around 6515 Å and then kept fixed during the convergence of the binary orbit. The strengths of lines of *star 2* were allowed to vary while they were kept constant for the much weaker lines of *star 1*. It resulted in decomposition of the profile of *star 1* into a double-peaked emission with a central reversal. All three decomposed line spectra are shown in Fig. 1 and the corresponding RV curves are in Fig. 2.

The KOREL solution led to the following orbital elements:

$$P = 12.93853 \text{ days}, \dot{P} = 0.0000005985 \text{ (both fixed)},$$

$$T_{\text{prim.ecl.}} = \text{HJD } 2449559.999,$$

$$K_1 = 42.1 \text{ km s}^{-1} \text{ and } K_2 = 186.8 \text{ km s}^{-1}$$

which leads to a mass ratio $M_1/M_2 = 4.432$, in an excellent agreement with the final orbital solution by Harmanec & Scholz (1993). It is true that the RV curve of *star 1* obtained by KOREL shows a great deal of scatter. Using the trial solutions with variable line strength we verified that this scatter can mostly be attributed to real secular changes in the intensity of the Si II emission. Additional scatter near phases of the primary eclipse can also be related to the presence of satellite lines and perhaps to the rotation effect. The secular line-strength variations could not be avoided with the currently available data since we had to combine spectra from several years to cover various orbital phases uniformly enough. It is clear that a better-defined RV curve of *star 1* could result from an application of KOREL to spectra secured during a dedicated campaign from several observatories in the course of one or two particular orbital cycles.

For the moment, we tentatively conclude that the Ondřejov spectra of β Lyr seem to confirm the system dimensions derived by Harmanec & Scholz (1993).

4. The gasdynamical modelling of circumstellar matter

We accept the standard model of β Lyr in which *star 2* is evolutionary unstable after the end of core hydrogen burning, fills the corresponding Roche lobe and loses matter towards *star 1*. To describe the gas flow in β Lyr we use the standard 3-D Euler equations in the reference frame corotating with the binary system. The Cartesian coordinate system used has the origin in the centre of *star 2* and is oriented as follows: X axis is directed towards *star 1* (the accretor), Z axis is directed along the vector of orbital rotation, and Y axis is directed against the sense of orbital motion of *star 2* around the centre of gravity. We adopt the following physical elements of the binary system: the mass-losing *star 2* fills its critical Roche lobe, having a mass of $M_2 = 2.98 M_\odot$ and effective temperature of $T_2 = 12000^\circ$; the accretor has the mass and radius of $M_1 = 13.2 M_\odot$ and $R_1 = 6 R_\odot$, respectively. The separation of the components is $A = 58.5 R_\odot$.

Gasdynamical simulations were conducted in the restricted region around the accretor. This region has a size $[A - D, A + D] \times [-D, D] \times [0, D]$, where D is a distance between the centre of the accretor and inner Lagrangian point L_1 . The computational domain (except the sphere which represents the accretor) is covered by a uniform grid of $61 \times 61 \times 17$ gridpoints in X , Y , and Z directions, respectively. Due to the symmetry around the orbital plane, all calculations were carried out only in the upper half-space. We would like to point out that using such a restricted computational domain allows one to reveal the main features of the flow structure in the vicinity of the accretor while far away from accretor the solutions obtained in restricted and larger regions may differ – c.f. Bisikalo et al. (1999).

The method of calculations was described in detail by Bisikalo et al. (1997), Bisikalo et al. (1998). To investigate the structure of the gaseous flows, we used a three-dimensional system of Euler equations and the equation of state of the ideal gas with the adiabatic index γ . The Euler equations describe the flow of unviscous gas. However, the resulting solution is affected by the numerical viscosity. In the model used, the numerical viscosity can be estimated as $\nu_{num} = c_s \Delta X$, where c_s is the sound velocity and ΔX is the size of the numerical mesh. In terms of the α -disc, the value of viscosity then corresponds to $\alpha \approx 0.05$. For practical reasons (to avoid too time-consuming calculations), the effects of radiative processes in the circumstellar matter were neglected and an adiabatic energy equation was used instead. To take the energy losses into account, at least approximately, we used the ratio of specific heats close to unity, $\gamma = 1.01$, which corresponds to a nearly isothermal case. Such a simplification is well known and has often been used by other investigators (see, e.g., Sawada et al. 1986, Bisikalo et al. 1995). The calculations were continued over 15 orbital periods until a steady state of the mass distribution within the system was achieved.

The overall structure of the gas flow in the orbital plane of the binary system is shown in Fig. 3 in a coordinate system corotating with the binary. A grayscale presentation is used to show the density distribution within the system. The velocity field

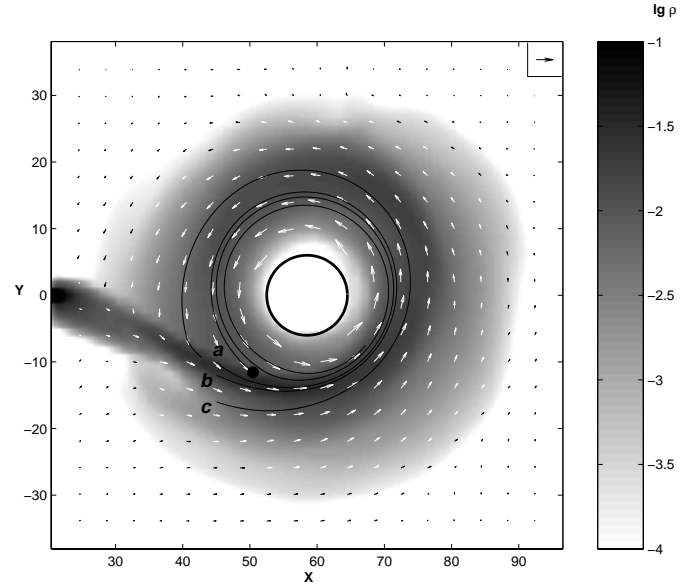


Fig. 3. Density distribution and the velocity vectors in the orbital plane of the binary system. Three particular flowlines, labelled ‘a’, ‘b’, and ‘c’ are also shown. The accretor is marked by the empty circle. The black dot indicates the position of the “optical centre” of the blue-shifted absorption lines, which was derived from the phase shift of their RV curves with respect to the RV curves of the binary components by Harmanec et al. (1996). These authors suggested that the spectral lines in question mainly arise from the self-absorption in one of the jet-like structures which they found from optical spectro-interferometry. A scaling vector in the upper right corner corresponds to velocity of 500 km s^{-1}

is also shown by velocity vectors. The binary rotates counterclockwise with an angular velocity Ω .

It should be noted that the particular value of the density has no influence on the solution, thanks to the scaling of the system of equations with respect to ρ (with a simultaneous scaling of pressure P). A value of $\rho(L_1) = 1$ was adopted, resulting in a density range from 10^{-4} to 10^{-1} in Fig. 3. To convert the dimensionless values to densities in absolute units, one has to multiply the values of Fig. 3 by the ratio of real \dot{M} to the calculated one (\dot{M}_{calc}). In our simulations \dot{M}_{calc} is defined as

$$\dot{M}_{calc} = \rho(L_1) \cdot C_s(L_1) \cdot S,$$

where $\rho(L_1) = 0.001 \text{ g mm}^{-3}$, $C_s(L_1) = 10 \text{ km s}^{-1}$ is the sound velocity, and S is the YZ surface of the grid mesh through which the gas is injected into the system. It is easy to estimate that the conversion factor for density is $\dot{M}/120$, where \dot{M} is in $M_\odot \text{ yr}^{-1}$. The observed orbital period is increasing at a rate of 18.9 s per year which implies \dot{M} of about $2 \cdot 10^{-5} M_\odot \text{ yr}^{-1}$ if an essentially conservative mass transfer is assumed.

Three particular flowlines, labeled “a”, “b” and “c”, are shown in Fig. 3. They illustrate the motion of the gas within the system. One sees that the matter of the stream is redistributed into two parts. The first one forms a quasi-elliptic accretion disc (flowline “a” shows that part of the stream which directly falls into the disc and has little effect on the disc size). The second part of the stream forms a circumstellar envelope around the

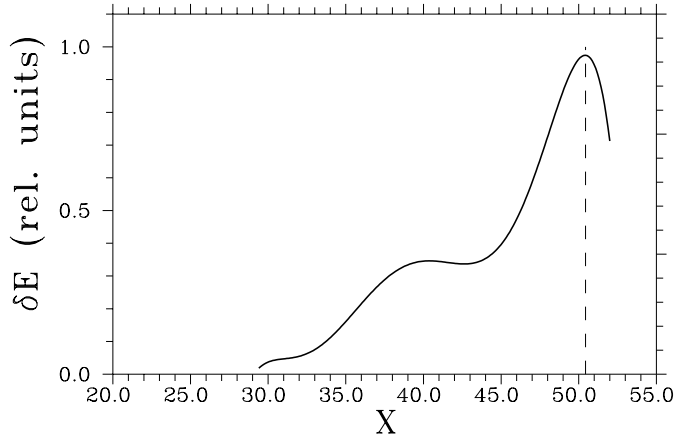


Fig. 4. Distribution of the specific rate of energy release along the shock wave in the direction of X axis in the orbital plane, normalized to unity. A dashed line marks the position of blue-shifted absorption lines originating in one of the jet-like structures found by Harmanec et al. (1996). The distances along the X axis are in units of R_{\odot} .

primary. As it is seen from the Fig. 3, a part of the flow (characterized by flowlines “ b ” and “ c ”) makes a full revolution around the accretor and mixes with the matter of the original stream from *star 2*. This matter *does not belong to the disc* since after interaction and mixing with the original stream it actually becomes a part of the stream itself. A part of the stream which does not interact with the disc at all immediately forms the outer parts of the circumstellar envelope.

The picture of the flow presented here shows that in the self-consistent solution, the accretion disc can be understood as that part of the gas stream which is gravitationally captured by the accretor. A numerical analysis of the 3-D gasdynamical solution also confirms an earlier conclusion by Bisikalo et al. (1997, 1998, 1999) that the gas stream (deflected under the action of the gas already present in the circumstellar envelope) approaches the disc tangentially and does not lead to the formation of the usually postulated “hot spot”. What actually happens is that the interaction between the gas from the circumstellar envelope and the stream results in the formation of an intensive shock wave, located along the stream edge which faces the accreting star.

As it is seen from the Fig. 3, the core (the densest parts) of the gas stream encircling the accretor interacts with the original stream just in the vicinity of the point labelled by a filled circle in Fig. 3. The position of this point

$$X = 50.4R_{\odot}, \quad Y = -11.55R_{\odot} \quad (2)$$

was adopted from Harmanec et al. (1996) who argued that the bulk of the $H\alpha$ absorption originated in one of the gaseous jet-like structures perpendicular to the orbital plane of the binary and emanating from an area near the point shown in Fig. 3. An analysis of the gasdynamical solution also shows that the main part of the energy release occurs indeed at the same area. This is documented in Fig. 4, where the distribution of the specific rate of the energy release in the shock wave along the X axis (normalized to unity), δE , is plotted. The vertical dashed line in

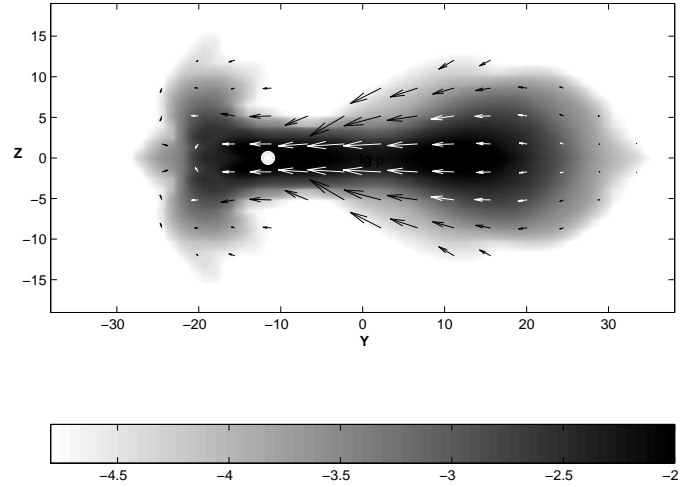


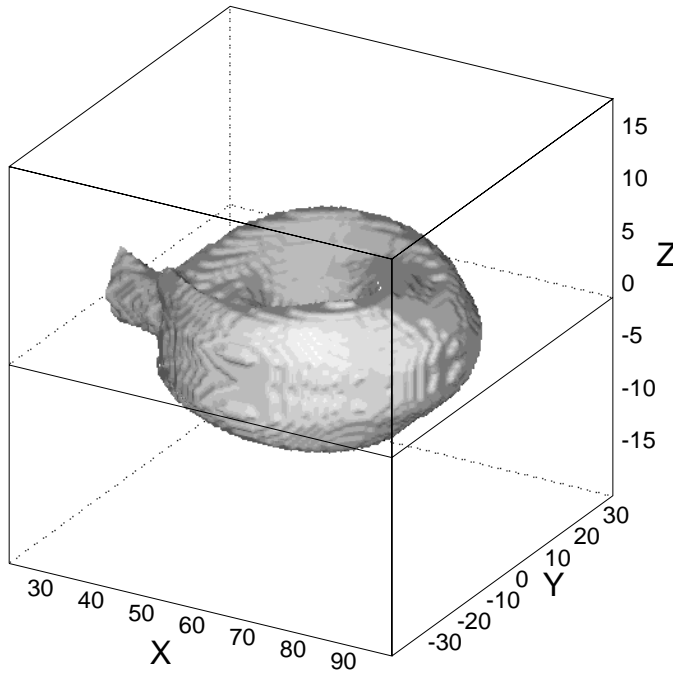
Fig. 5. Density distribution and velocity vectors in the YZ plane at $X = 50.4$. The point from which the jet-like structures emanate according to Harmanec et al. (1996) is denoted by a white circle.

Fig. 4 denotes the position of the “jets” which clearly coincides with the maximum rate of the energy release.

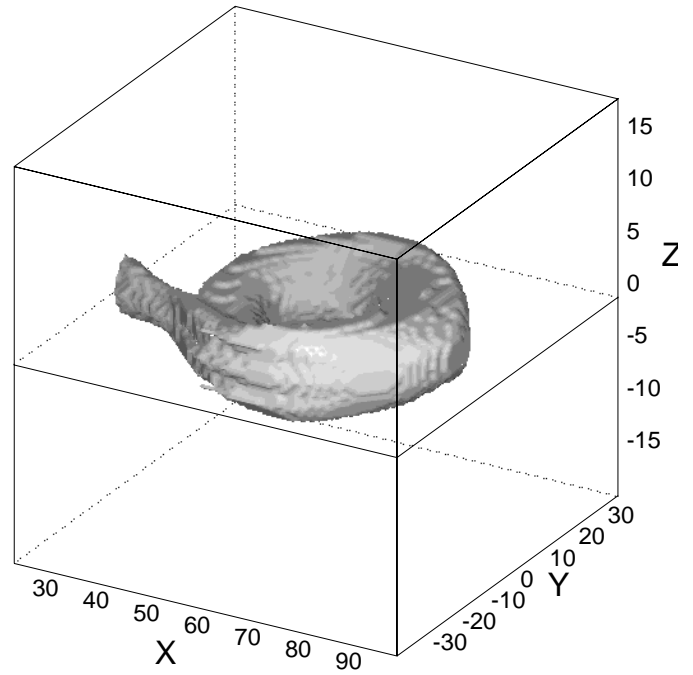
An analysis of the flow structure in YZ plane shows that a part of the circumstellar envelope interacts with the (denser) original gas stream and is deflected away from the orbital plane. This naturally leads to the formation of gaseous structures moving perpendicularly to orbital plane. They are well seen in Fig. 5, where the density distribution and velocity vectors in YZ plane are shown. The point defined by (2) is shown. It is seen that the calculated structures perpendicular to the orbital plane emanate from an area whose distance from the accretor is somewhat larger than that of the point derived by Harmanec et al. (1996).

The velocities along the Z -direction obtained from the gasdynamical solution are of the order of $\sim 100 \text{ km s}^{-1}$. The mean RV of the blue-shifted absorption lines of $H\alpha$ and He I 6678 was found to be -82 and -84 km s^{-1} , respectively, by Harmanec et al. (1996). For the binary inclination of 83° it translates into a true outflow velocity of the material in which these lines originate of $\sim 680 \text{ km s}^{-1}$. This is much higher velocity than the outflow velocity of the calculated structures. It appears, therefore, that one cannot directly identify the absorption lines with the calculated structures.

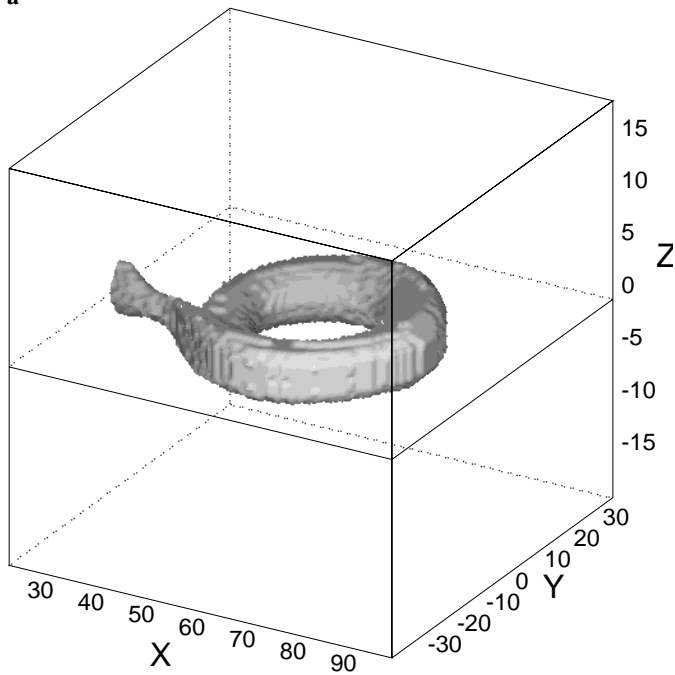
There can be different solutions to this problem. One possibility is that the current gasdynamical model does not predict the outflow velocities well enough because of all physical simplifications inherent to it. Another one is to assume that the observed absorption lines are in fact formed by contributions from different parts of circumstellar matter. Even the gasdynamical model presented here indicates that the polar regions of *star 1* are not completely hidden inside the envelope. Therefore, the presence of a normal stellar wind emanating from the polar regions of an early-B *star 1* is to be expected. This wind must also move mainly along the directions perpendicular to the orbital plane since in all other directions it interacts with the envelope and loses its identity. It is conceivable, therefore, that the blue-shifted absorption lines are partly due to this wind, as already



a



b



c

Fig. 6a – c.

a A bird-eye view of the density iso-surface at the level $\rho = 1 \cdot 10^{-3} \rho(L_1)$. All coordinates are scaled in units of R_\odot

b A bird-eye view of the density iso-surface at the level $\rho = 3 \cdot 10^{-3} \rho(L_1)$. All coordinates are scaled in units of R_\odot

c A bird-eye view of density iso-surface at the levels $\rho = 5 \cdot 10^{-3} \rho(L_1)$. All coordinates are scaled in units of R_\odot

remarked by Harmanec et al. (1996). A future analysis of very high-resolution spectra could show if such an interpretation is tenable or not.

Whatever the true solution to the velocity problem will be, the 3-D gasdynamical calculations presented here undoubtedly suggest that the gas from the circumstellar envelope which is deflected away from the orbital plane after interaction with the incoming stream may play an important role in β Lyr. The analysis of flowlines shows that this matter does not belong to

the accretion disc. A part of it directly leaves the system while the other one moves in the orbital plane, encircles the accretor and then collides with the stream. Let us call this part of the envelope a “halo”. Following to Bisikalo et al. (1999), one can define “halo” as that matter which:

- encircles the accretor being gravitationally captured;
- does not belong to the accretion disc;
- interacts with the stream (collides with it and/or overflows it);

- after the interaction either becomes a part of the accretion disc or leaves the system.

The presence of the “halo” in the gasdynamical model of β Lyr is well seen in Fig. 6, where the bird-eye view of density iso-surfaces at the levels of $\rho = 1 \cdot 10^{-3} \rho(L_1)$, $\rho = 3 \cdot 10^{-3} \rho(L_1)$, and $\rho = 5 \cdot 10^{-3} \rho(L_1)$ are shown.

Note that the presence of a “light-scattering corona” in β Lyr was recently postulated by Linnell et al. (1998) on the basis of a different line of reasoning. The above gasdynamical analysis seems to corroborate their suggestion and demonstrates the existence of a rather dense “halo” around *star 1* of β Lyr.

5. Conclusions

The main result of this study is the finding that a self-consistent 3-D gasdynamical simulation of the gas stream in a binary system with the basic physical properties similar to the observed properties of β Lyr is indeed able to explain the formation of the principal observed components of the circumstellar matter mentioned in Sect. 2: an accretion disc, a scattering envelope and even the jet-like structures perpendicular to the orbital plane. The agreement is very good on a qualitative level. In some aspects, like the estimated position of the root of the jets in the orbital plane, the agreement is remarkable even on a quantitative level.

Acknowledgements. Our thanks are due to Drs. J. Horn, P. Koubský, J. Kubát, V. Šimon, P. Škoda, S. Štefl, and M. Wolf who at our request obtained some of the Ondřejov spectrograms of β Lyr. D.Bisikalo and O.Kuznetsov gratefully acknowledge the hospitality of the staff of the Ondřejov Observatory during their visit there. We acknowledge the comments by an anonymous referee which helped us to organize the text in a more consistent and logical way.

This study was initiated during the visit of D.Bisikalo and O.Kuznetsov to the Ondřejov Observatory. Their visit was supported from the research grant 205/96/0162 of the Granting Agency of the Czech Republic to P. Harmanec. The research of P. Hadrava and P. Harmanec was supported by research grants 205/96/0162 of the Granting Agency of the Czech Republic and A3003805 of the Granting Agency of the Academy of Sciences of the Czech Republic. This work was also supported in part by Russian Foundation of Basic Research (grant 99-02-17619) and by a grant of the President of Russia (99-15-96022).

References

- Baxandall F.E., Newall H.F., Stratton F.J.M., 1930, *Annals Solar Phys. Obs. Cambridge Vol. 2 Part I*, 1
- Bélopolsky A., 1893a, *Bull. Acad. Impèr. Sciences St.-Petersbourg* 7, 423
- Bélopolsky A., 1893b, *Mem. Soc. Spett. Ital.* 22, 101
- Berghöfer T.W., Schmitt J.H.M.M., 1994, *A&A* 292, L5
- Bisikalo D.V., Boyarchuk A.A., Kuznetsov O.A., Chechetkin V.M., Popov Yu.P., 1995, *AZh* 72, 367 = *Astron. Report* 39, 325
- Bisikalo D.V., Boyarchuk A.A., Kuznetsov O.A., Chechetkin V.M., 1997, *AZh* 74, 880 = *Astron. Report* 41, 786
- Bisikalo D.V., Boyarchuk A.A., Chechetkin V.M., Kuznetsov O.A., Molteni D., 1998, *MNRAS* 300, 39
- Bisikalo D.V., Boyarchuk A.A., Kuznetsov O.A., Chechetkin V.M., 1999, *AZh*, (in press)
- Burnashev V.I., Skulskij M.Yu., 1978, *Izv. Krym Astrophys. Obs.* 58, 64
- Curtiss R.H., 1911, *Publ. Allegheny Obs.* 2 (No.11), 73
- Hadrava P., 1995, *A&AS* 114, 393
- Hadrava P., 1997, *A&AS* 122, 581
- Harmanec P., 1990, *A&A* 237, 91
- Harmanec P., 1992, *A&A* 266, 307
- Harmanec P., Scholz G., 1993, *A&A* 279, 131
- Harmanec P., Morand F., Bonneau D., et al., 1996, *A&A* 312, 879
- Hoffman J.L., Nordsieck K.H., Fox G.K., 1998, *AJ* 115, 1576
- Jameson R.F., King A.R., 1978, *A&A* 63, 285
- Linnell A.P., Hubeny I., Harmanec P., 1998, *ApJ* 509, 379
- Perryman M.A.C., Høg E., Kovalevsky J., Lindegren L., Turon C., 1997, *ESA SP-1200, The Hipparcos and Tycho Catalogues*
- Plavec M.J., 1985, In: Eggleton P.P., Pringle J.E. (eds.) *Interacting Binaries*. Reidel, Dordrecht, p. 155
- Sahade J., 1966, *Trans. IAU Vol. XIIB*, 494
- Sahade J., 1980, *Space Sci. Rev.* 26, 349
- Sahade J., Huang S.-S., Struve O., Zebergs V., 1959, *Trans. Amer. Philosoph. Soc. New Ser.* 49, Part 1, 1
- Sawada K., Matsuda T., Hachisu I., 1986, *MNRAS* 219, 75
- Secchi A., 1867, *Astron. Nachr.* 68, 63
- Skulskij M.Yu., 1975, *AZh* 52, 710
- Skulskij M.Yu., 1992, *Pisma AZh* 18, 711
- Skulskij M.Yu., Topilskaya G.P., 1991, *Pisma AZh* 17, 619
- Struve O., 1934, *Observatory* 57, 265
- Struve O., 1941, *ApJ* 93, 104
- Wilson R.E., 1974, *ApJ* 189, 319